Microchimica Acta (2019) 186: 43
https://doi.org/10.1007/s00604-018-3162-2

ORIGINAL PAPER

A split aptamer-labeled ratiometric fluorescent biosensor for specific detection of adenosine in human urine

Junhui You[1] · Zhengyi You[1] · Xin Xu[1] · Jiangrong Ji[1] · Tian Lu[1] · Yuhong Xia[1] · Lipin Wang[1] · Liying Zhang[1] · Shuhu Du[1]

Received: 13 September 2018 / Accepted: 9 December 2018 / Published online: 19 December 2018

Abstract

A dual-emission ratiometric fluorometric aptasensor is presented for highly specific detection of adenosine. An adenosine binding aptamer (ABA) was split into two halves (termed as ABA1 and ABA2). ABA1 was covalently bound to blue-emitting carbon dots (with excitation/emission maxima at 365/440 nm) as responsive fluorophore (referred to as ABA1-CDs). ABA2 was linked to red-emitting silica-coated CdTe quantum dots (with excitation/emission maxima at 365/613 nm) acting as internal reference and referred to as ABA2-QDs@SiO_2. Upon addition of graphene oxide, the fluorescence of ABA1-CDs is quenched. After subsequent addition of ABA2-QDs@SiO_2 and different amounts of adenosine, the blue fluorescence is recovered and causes a color change from red to royal blue. The method represents a ratiometric turn-on assay for visual, colorimetric and fluorometric determination of adenosine. The limit of detection is as low as 2.4 nM in case of ratiometric fluorometry. The method was successfully applied to the determination of adenosine in (spiked) human urine. Recoveries range from 98.8% to 102%.

Keywords Nanoprobe · Fluorescence resonance energy transfer · Carbon dots · CdTe quantum dots · Graphene oxide · Visual detection · Adenosine

Introduction

Adenosine is a biological cofactor and modulator with potent vasodilator and antiarrhythmic activities. It also is a potential cellular tumor marker [1]. The determination of adenosine is of great value in clinical diagnosis. Various analytical methods have been developed for the monitoring of adenosine, including voltammetric [2], capillary electrophoresis [3], mass spectrometry [4], surface-enhanced Raman spectroscopy (SERS) [5], and so on. However, most of them require expensive instrumentation and labor-intensive sample preparations, and are often unavailable for the on-site detection, especially in developing countries. Thus, there is a great demand for developing a rapid and inexpensive method for the on-site analysis of trace adenosine in the biological fluids, motivating many researchers to fabricate new miniature fluorescent/chemical nanoprobe.

Fluorescent nanoprobes possess many outstanding advantages, which include rapid response and high sensitivity. Carbon dots (CDs) and quantum dots (QDs), as novel fluorescent probes, have attracted tremendous attentions in last decades due to its good photochemical stability, strong fluorescence signals, superior biocompatibility and low toxicity compared with traditional organic dyes. Nowadays, a variety of analytical strategies have been applied in the detections of Aflatoxin B1 via CDs-functionalized MnO_2 nanosheets [6], Pb(II) with P-GO@QDs [7], dopamine using aptamer labeled CDs [8], adenosine by aptamer-CuZnInS QDs conjugation [9], and so on. However, most of aptasensors are single-emission, which may be influenced by experimental conditions such as instruments, excitation intensity, emission collection efficiency and environmental factors, finally resulting in poor accuracy. Compared with the single-emission aptasensor, dual-emission fluorescent aptasensors have several merits

Electronic supplementary material The online version of this article (https://doi.org/10.1007/s00604-018-3162-2) contains supplementary material, which is available to authorized users.

✉ Shuhu Du
shuhudu@njmu.edu.cn

[1] School of Pharmacy, Nanjing Medical University, Nanjing 211166, Jiangsu, China

such as the wider dynamic response range, improved sensitivity and accuracy. Therefore, it is an urgent demand to design a dual-emission ratiometric fluorescent aptasensor for the detection of adenosine.

We report here on a dual-emission ratiometric fluorescent aptasensor for highly sensitive and specific detection of adenosine. In the preparation procedure of this aptasensor, adenosine binding aptamer (ABA) was first split into two flexible single strands (termed as ABA1 and ABA2). ABA1 was covalently attached to blue-emitting CDs while ABA2 was linked to red-emitting silica-coated CdTe quantum dots (QDs@SiO_2), corresponding forming ABA1-CDs as a reporter signal and ABA2-QDs@SiO_2 as a reference signal. In practical detection, when ABA1-CDs was dropped into graphene oxide (GO) aqueous solution, fluorescence of CDs labeled ABA1 was quenched due to fluorescence resonance energy transfer (FRET) between CDs and GO. After simultaneous addition of ABA2-QDs@SiO_2 and adenosine, the fluorescence of ABA1-CDs was recovered. The method was finally applied for the analysis of adenosine in urine samples of healthy humans and lung cancer patients. A satisfactory result was obtained.

Experimental

Materials

Tellurium powder, $NaBH_4$, $CdCl_2$•$2.5H_2O$, sulfuric acid (98%), NaOH, ethanol (95%), citric acid, tetraethylorthosilicate (TEOS), 3-aminopropyltriethoxysilane (APTES) were purchased from Sinopharm Chemical Reagent Co., Ltd. (Shanghai, China, http://www.sinoreagent.com/). Ethylenediamine was supplied by Macklin Biochemical Co., Ltd. (Shanghai, China, http:// www.chemicalbook.com/). 3-Mercaptopropionic acid (MPA) and HEPES were obtained from Sigma-Aldrich. N-(3-dimethylaminopropyl)-N-ethylcarbodiimide hydrochloride (EDC), N-hydroxysuccinimide (NHS) and graphene oxide (GO) were purchased from Aladdin Chemistry Co., Ltd. (Shanghai, China, http://www.aladdine.com/). All reagents were of analytical grade and without any further purification. Ultrapure water (18.2 MΩ cm) was prepared by a Millipore water purification system (Milfords, MA, USA, http://millipore.bioon.com.cn/).

All the oligonucleotide sequences used in this study were synthesized and purified through HPLC by Sangon Biotechnology Inc. (http://www.sangon.com/) For adenosine, the split aptamers sequence information were list as follows: 5'-NH_2-C_6-TT TTT TAC CTG GGG GAG TAT-3′, denoted as adenosine binding aptamer 1 (ABA1) and 5'-COOH-T TTT TTT GCG GAG GAA GGT-3′, denoted as adenosine binding aptamer 2 (ABA2).

Two participants (patients with lung cancer from the Sir Run Run Hospital of Nanjing Medicine University) agreed and succeeded in providing suitable urine samples. Informed consent forms were renounced because these samples were anonymized. Moreover, normal urine samples were collected from two healthy volunteers. All samples were stored at −70 °C until analysis.

Apparatus

Fluorescence and UV–vis absorption spectra were recorded by Hitachi F-7000 fluorescence instrument (Hitachi, Japan, http://www.hitachi.com/) and Shimadzu UV-2450 spectrophotometer (Shimadzu, Japan, http://www.shimadzu.com.cn/), respectively. A JEOL JEM-2100 transmission electron microscope (TEM) instrument (Tokyo, Japan, http://www.jeol.co.jp/en/products/detail/JEM-2100F.html) was used to observe the morphology of nanoparticles. FT-IR spectra were recorded on a TENSOR 27 spectrometer (Bruker, Germany, http://www.bruker.com/) with a resolution of 2 cm^{-1} and a spectral range of 4000–400 cm^{-1}. Fluorescent photos were taken under an AGL-9406 UV lamp with a Canon 600D digital camera. The combination between aptamer and nanomaterials was confirmed by 4.0% agarose gel electrophoresis with 0.5 TBE buffer at 100 V for 60 min by Tanon EPS-300 (China, http://www.biotanon.com/). To assess accuracy of the method, urine samples were also analyzed on HPLC (Agilent, USA, http://www.agilent.com/).

Preparations of CDs, QDs and QDs@SiO_2

The CDs, QDs and QDs@SiO_2 were prepared as described in our previous work [10–12]. See the details of synthesis in the Electronic Supp. Material (ESM).

Synthesis of split aptamer-labeled nanoparticles

The conjugations between nanoparticles and split aptamers were synthesized by the method of previous literature [13]. To obtain ABA1-CDs, 20 μL of CDs solution was first added into 30 μL of mixed solution of EDC and NHS (the concentrations of EDC and NHS were set at 200 $\mu g \cdot mL^{-1}$, respectively). The mixture was sonicated for 20 min. Afterwards, 10 μL of the mixture solution with carboxy-stabilized CDs was added to 1 mL of 5 μM ABA1 with HEPES buffer (pH = 7.4). The solution was further incubated for 2 h at 25 °C. Finally, the unreacted aptamer and excess reagents were removed by filtration in cutoff spin filters at 5000 rpm for 10 min. ABA2-QDs@SiO_2 were synthesized by the similar procedures.

Determination of adenosine in aqueous solution

75 μL of ABA1-CDs solution was first added into 4 μL of GO solution under gentle shaking. The mixing solution was then incubated at room temperature. Subsequently, 1 μL of adenosine solution (with different concentrations) and 20 μL ABA2-QDs@SiO_2 solution were added into the above mixing solution. Finally, the fluorescent spectra were recorded with a spectrometer, and the signal output values were calculated according to the relative fluorescent intensity (I_{440}/I_{613}), in which I_{440} and I_{613} represented the fluorescence of the ABA1-CDs and ABA2-QDs@SiO_2, with the excitation of 365 nm.

Analysis of urine samples

Urine samples were filtered through a 0.45 μm supor filters to remove any particulate suspension, and then stored in refrigerator at −70 °C until further analysis. Urine samples (1 μL) were detected as described above.

Results and discussion

Characterization of nanoparticles

The properties of CDs, QDs and QDs@SiO_2 were characterized by TEM, UV − vis absorption and fluorescence spectroscopy. For CDs, a good monodispersity with a diameter of ~3 nm is displayed in Fig. 1a. Fig. 1b (curve a) exhibits an emission peak at 440 nm with an excitation of 365 nm, and a bright blue fluorescence is observed under a 365 nm UV lamp (inset a in Fig. 1b). As shown in Fig. 1c and e, the used QDs have an average particle size of ~3 nm and the QDs@SiO_2 have an average particle size of ~40 nm, whose core-shell structure with an average shell thickness of ~12 nm is clearly revealed by the observation of TEM. The corresponding two fluorescence emission peaks located at 607 and 613 nm (the red curve in Fig. 1d and f). A bright red and a dark red fluorescence are observed under a 365 nm UV lamp (inset a in Fig. 1d and f), respectively. To further confirm the surface status information on CDs, QDs and QDs@SiO_2, FT-IR measurements were also carried out. In Fig. S1 (curve a), the CDs displays characteristic peaks at 1570 cm^{-1} and 1379 cm^{-1}, indicating that there are carboxy groups at the surface of the CDs. As shown in Fig. S1 (curve b), the appearance of two characteristic bands at 1562 cm^{-1} and 1394 cm^{-1} as the carboxy vibration of MPA demonstrates that MPA covalently binds to the surface of QDs [14]. In Fig. S1 (curve c), QDs@SiO_2 show a strong absorption at 1089 cm^{-1} (attributed to the antisymmetric stretching vibration of Si − O − Si), two absorptions at 3462 cm^{-1} and 3419 cm^{-1} (attributed to asymmetric and symmetric stretching vibrations of N-H) and two weak absorptions at 1562 cm^{-1} and 1394 cm^{-1}, suggesting that SiO_2 is successfully coated on the surface of QDs [15–17].

Characterization of split aptamer-labeled nanoparticles

The 27-nt anti-adenosine aptamer was chosen as a representative for biological functionalization of nanoparticles (see the detailed statements in ESM). Fig. S2a shows that the integer aptamer is designed into two pieces of sequences. The fluorescent nanoparticles (with –COOH or $–NH_2$) and spilt aptamer (with $–NH_2$ or –COOH) are bridged with a general EDC-NHS coupling system. The coupling system further was confirmed by agarose gel electrophoresis analysis. It is found that the band of ABA1-CDs was retarded compared with other lanes (Fig. S2b). The results clearly demonstrated that ABA1 was successfully covalently linked to CDs. Likewise, similar results were also obtained for the ABA2-QDs@SiO_2 (Fig. S2c).

Mechanism of ratiometric fluorescent aptasensor for adenosine

The mechanism of the fluorescent aptasensor for ratiometric detection of adenosine based on the GO platform is showed in scheme 1. As mentioned above, the fluorescent aptasensor is designed into two separated moieties (ABA1-CDs and ABA2-QDs@SiO_2). ABA1-CDs and GO readily form stable ABA1-CDs/GO complex in aqueous solution through strong π stacking interaction between nucleotide bases and honeycomb lattices of GO, which is accompanied by a significant fluorescence quenching. In order to further explore the mechanism of fluorescence quenching, the Stern-Volmer (SV) quenching constants were measured based on ABA1-CDs versus concentration of GO at three temperatures (288, 298 and 308 K). The SV equation is defined as $F_0/F = 1 + K_{sv}C$ (C is the concentration of quencher GO, K_{sv} is the SV quenching constants, F_0 and F are the fluorescence intensity of the ABA1-CDs without GO and with different concentrations of GO, respectively). As previously reported literature [18], K_{sv} will decrease with rise of temperature in static quenching and the reverse in dynamic quenching. Fig. S3 shows that K_{sv} is inversely proportional to the temperature, revealing that the ABA1-CDs/GO system is a static quenching process. In the absence of adenosine, when ABA2-QDs@SiO_2 are added, no apparent fluorescence enhancement signal is observed. However, in the presence of adenosine, the two pieces reassemble into intact tertiary structure and the sandwich complex (ABA1-CDs/adenosine/ABA2-QDs@SiO_2) induced by adenosine aptamer fragments can be formed. As a consequence, a significant fluorescence restoration occurs because ABA1-CDs are far away from the GO surface and the energy

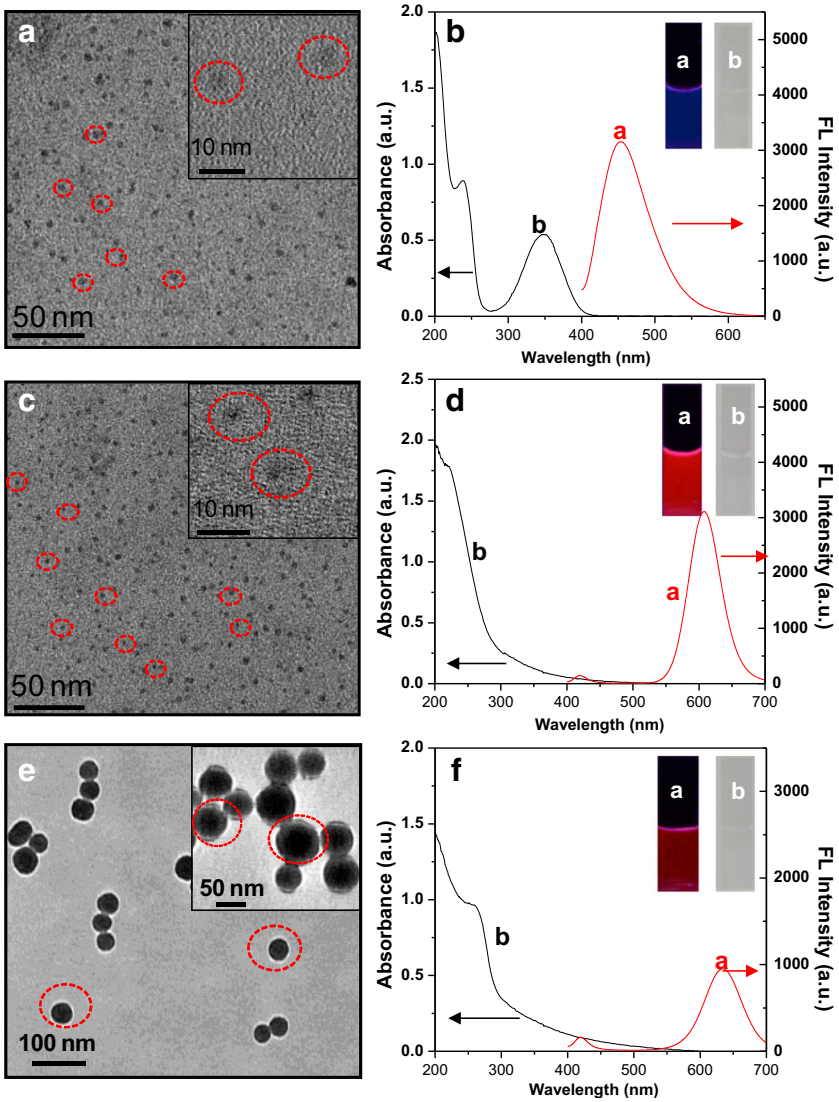

Fig. 1 TEM images of (**a**) CDs, (**c**) QDs and (**e**) QDs@SiO_2 (The insets red circles represent nanoparticles). UV-vis absorbance and fluorescence emission of (**b**) CDs, (d) QDs and (**f**) QDs@SiO_2 (insets a and b show the corresponding colors under 365 nm UV lamp and daylight)

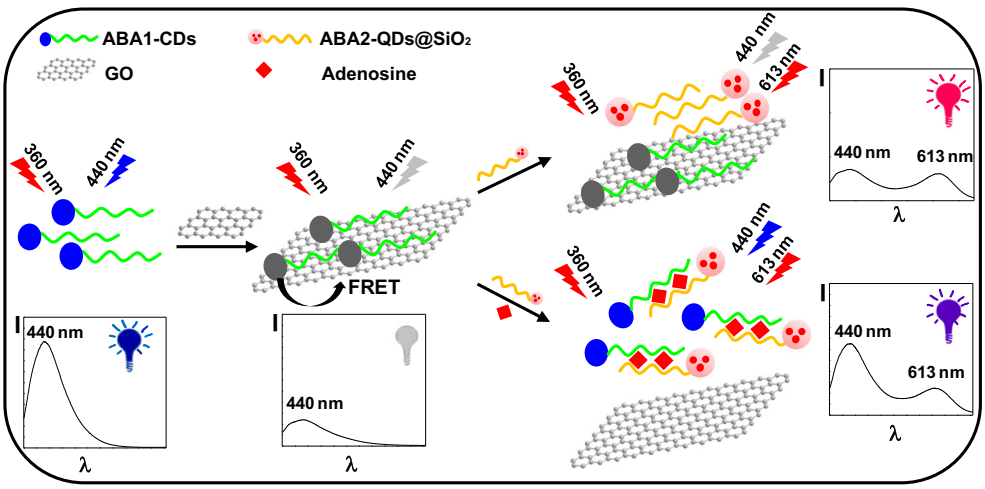

Scheme 1 Mechanism for fluorescence turn-on and ratiometric detection of adenosine by using aptasensor and GO

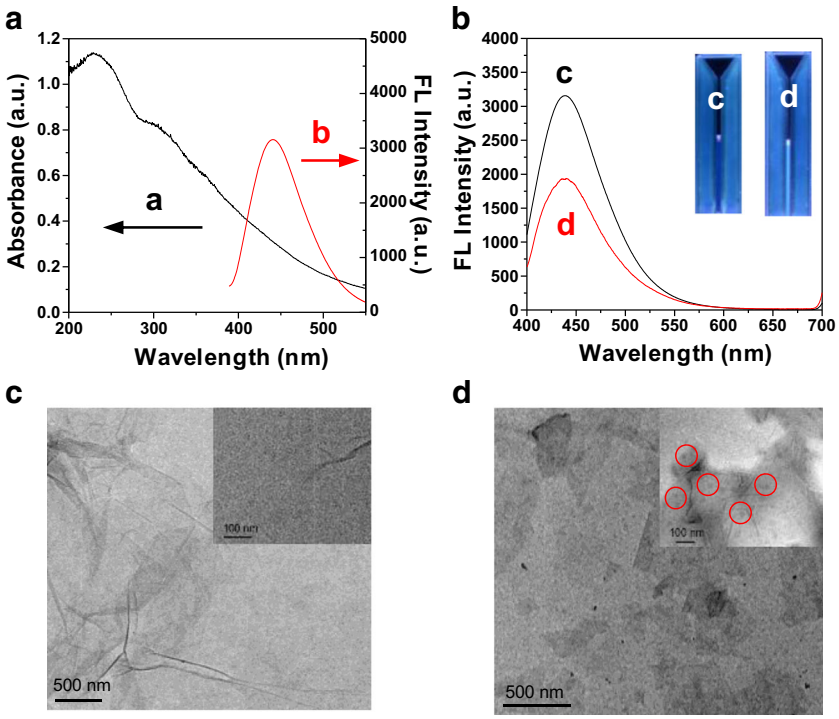

Fig. 2 **a** UV–vis absorption spectrum of GO and fluorescence emission spectrum of ABA1-CDs. **b** Fluorescence emission spectra of ABA1-CDs and ABA1-CDs/GO. The insets show the corresponding colors of ABA1-CDs before and after addition of GO under a 365 nm UV lamp. **c**, **d** TEM images of GO before and after addition of ABA1-CDs, respectively (inset: red circles represent nanoparticles)

transfer efficiency decreases [19]. While the QDs are stabilized in the interior of SiO_2 (whose thickness is larger than typical Förster distance 8 nm [20], avoiding the FRET), and the fluorescence of ABA2-QDs@SiO_2 keeps constant during the process, which plays a role of internal standard. Thus, the fluorescence "turn-on" switch concept by the fluorescence signal readout of ABA1-CDs and ABA2-QDs@SiO_2 is utilized for the ratiometric detection of adenosine.

The above concept for the detection of adenosine was further evidenced by the UV-vis and fluorescence spectroscopies. As shown in Fig. 2a, GO has a broad absorption from 200 to 550 nm, and its absorption spectrum overlaps with the fluorescence emission spectrum of ABA1-CDs. When ABA1-CDs was absorbed on the surface of GO, the fluorescence of ABA1-CDs would be quenched owing to FRET (curve d in Fig. 2b) [21], and the color of system changed from deep blue to light sky blue (the inset of Fig. 2b). The TEM observations also revealed that ABA1-CDs can adhere onto the surface of the GO sheet by the π stacking interaction (Fig. 2c and d).

Optimization of method

The following parameters were optimized: (a) incubation time; (b) aptamer concentration; (c) temperature; (d) pH value; (e) the amount of GO and (f) the response time of the aptasensor [22–24]. Respective data and Fig. S4–6 are given in the ESM. The following experimental conditions were found to give best results: (a) optimal incubation time: 2 h; (b) aptamer concentration: 5 μM; (c) temperature: 25 °C; (d)

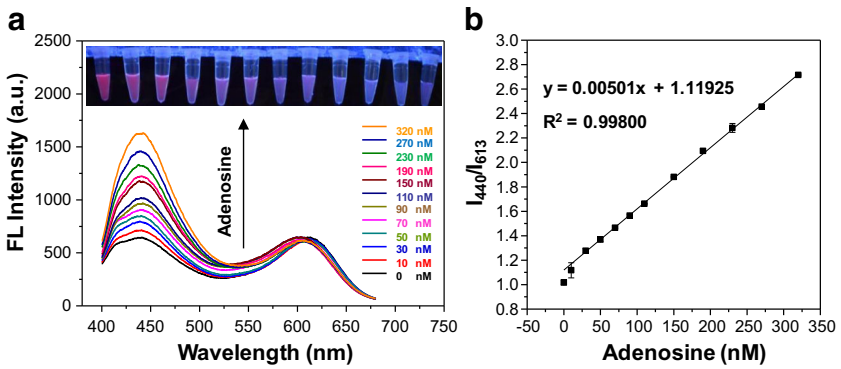

Fig. 3 **a** Fluorescence emission spectra (λ_{ex} = 365 nm and λ_{em} = 440/613 nm) of ratiometric fluorescent aptasensor with the increase of adenosine concentrations. The inset photos show the evolution of corresponding colors under 365 nm UV lamp. **b** The linear correlation of fluorescent intensity ratio (I_{440}/I_{613}) with adenosine concentrations from 0 to 320 nM

Table 1 Comparison of adenosine detection results in the previous and present works

Detection method	Linear range	LOD	Fluorescence response	Colorimetry-based quantification	Sample	Ref.
Electrochemistry	1–270 μM	0.16 μM	–	No	Urine	[2]
Capillary electrophoresis	5–200 μM	2.2 μM	–	No	Cell	[3]
Mass spectrometry	2.5–50 μM	0.48 μM	–	No	Cell	[4]
SERS	0.1–10,000 μM	0.1 μM	–	No	–	[5]
Fluorescence	10–500 nM	4.2 nM	"Turn on"	No	–	[26]
Fluorescence	0.1–5.0 nM	80 pM	"Turn on"	No	Yogurt	[27]
Fluorescence	0.1–30 nM	60 pM	"Turn off"	No	Urine	[28]
Fluorescence	0.1–100 μM	89 nM	Enhancement	No	Urine/ Serum	[29]
Colorimetric assay	5–1000 nM	0.13 nM	–	Yes	–	[30]
Fluorescence	12–200 nM	12 nM	"Turn off"	No	–	[31]
Fluorescence	0–320 nM	2.4 nM	"On-off-on"	Yes	Urine	This work

"-" represents which had not been mentioned in the related literature

Best sample pH value: 7.4; (e) the amount of GO: 0.03 mg·mL^{-1} and (f) the response time of the aptasensor: 30 min.

Sensitivity and selectivity

Prior to the sensitivity assay, the stabilities of this aptasensor system were first investigated by fluorescence spectroscopy. As shown in Fig. S7a and b, fluorescent intensities of ABA1-CDs (at 440 nm) and ABA2-QDs@SiO_2 (at 613 nm) were stable within 2 h. Moreover, after being quenched by GO, the fluorescent of the ABA1-CDs was stable (Fig. S8a), whereas ABA2-QDs@SiO_2 had no obvious fluorescent response to GO within 40 min (Fig. S8b), providing a reliable reference signal for ratiometric detection of adenosine. Fig. 3a shows the fluorescent spectra of ratiometric fluorescent aptasensor exposed to the aqueous solution containing different amounts of adenosine perform at excitation wavelength 365 nm and emission wavelength range 400–680 nm. Evidently, the emission intensity at 440 nm is gradually turned on due to switching off the FRET process. The results display that the increase of adenosine to the ratiometric fluorescent aptasensor solution indeed induces an obvious fluorescence enhancement at 440 nm whereas the emission intensity at 613 nm is still unchanged. Consequently, the emission intensity ratio (I_{440}/I_{613}) is gradually increased with increase of adenosine concentrations. When adenosine was added up to 320 nM, it was observed that the ratiometric fluorescent intensity was enhanced about three times. This turn-on and ratiometric fluorescence enhancement can also be visualized with the solution color changes from red to royalblue under a 365 nm UV lamp (the inset of Fig. 3a), which offers a nice opportunity for the bare eye detection without the need for expensive instrument except for a small UV lamp as an excitation light source. Because a ratiometric fluorescent assay possesses superior ability of quantitative assay based on its self-calculation of dual emission intensity ratios which is independent of the probe concentration, the plot of I_{440}/I_{613} to adenosine concentration yields a calibration plot that gives linear relationship with the a correlation coefficient of 0.998 (Fig. 3b). The detection limit is determined to be 2.4 nM based on the definition of 3 times the deviation of the blank signal (3σ, where σ is the standard deviation for ten blank measurements), which is about 3 orders of magnitude lower than that reported in the previous literature by single-emission [25]. Compared with the other reported methods, our method mainly possesses two advantges, such as excellent anti-interference ability (using the ratio at two different emission wavelengths, instead

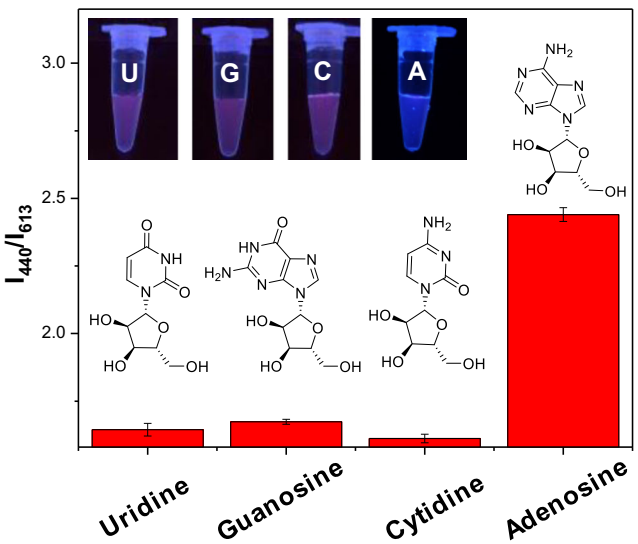

Fig. 4 Selectivity of ratiometric fluorescent aptasensor upon the addition of various nucleoside analogs (U: uridine, G: guanosine, C: cytidine, A: adenosine). Four nucleoside analogs are tested under the same conditions. Adenosine concentration is 270 nM, and others are 270 μM. The insets show the corresponding fluorescent photos taken under 365 nm UV lamp

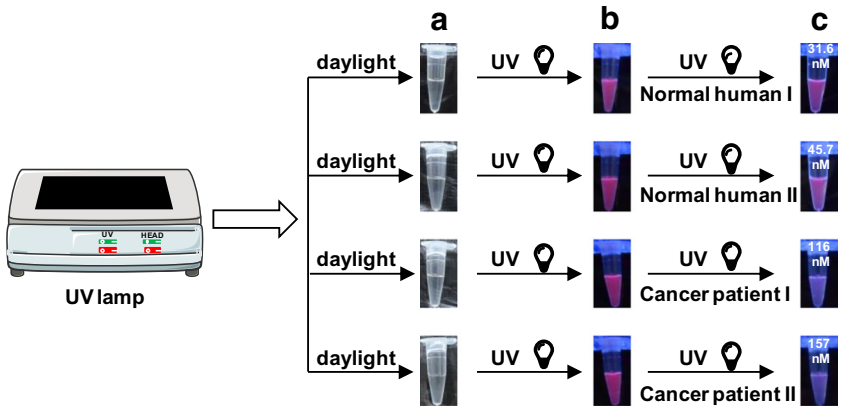

Fig. 5 The visual detection of adenosine in urine samples from normal humans and lung cancer patients. Each sample was diluted 100-fold after the addition into the solution of ratiometric fluorescent aptasensor. The photos of ratiometric fluorescent aptasensor were taken (**a**) under daylight, (**b**) under UV lamp and (**c**) after the addition of real urine samples under UV lamp

of the absolute intensity at only one wavelength, which can provide a built-in correction) and wide color variation (from red to purple to slateblue) (Table 1).

Moreover, the selectivity of ratiometric fluorescent aptasensor was evaluated by the test of other nucleoside analogs with concentrations of 270 μM. When three nucleoside analogs including uridine, guanosine and cytidine were added into the assay system, none of the three nucleosides produced statistically significant fluorescence enhancement and the fluorescent color of solution was still the original red under a UV lamp (Fig. 4) even though the each concentration was a 1000 times more than that of adenosine. In contrast, obvious change happened in the fluorescence intensity ratio and color after adding adenosine in the assay system (the inset of Fig. 4), suggesting that the ratiometric fluorescent aptasensor had an excellent selectivity to adenosine.

Analytical application in real samples

On the basis of the above results, the method was applied for the analysis of adenosine in real urine samples (collected from two healthy volunteers and two patients with lung cancer). In general, the concentration of adenosine in normal human urine is in the range of 2.0 to 7.0 μM [32, 33], and the reference limit of adenosine in lung cancer patient is higher than 7.0 μM [34]. As shown in Table S1, adenosine concentrations in four urine samples which were diluted 100-fold were highly accord with those from the HPLC method. Interestingly, the concentrations of adenosine from normal human urine (3.16, 4.57 μM) correspond to pink, whereas the concentrations of adenosine from lung cancer patient urine (11.6, 15.7 μM) correspond to slateblue, suggesting a discernible dosage capability by the bare eye (Fig. 5). The recoveries of adenosine ranged from 98.8% to 102% with the relative standard deviation (RSD) less than 5%, satisfying the requirements of the practical application with excellent precision and reliability. Besides, the concentrations of adenosine in urine samples from lung cancer patients were significantly higher than those of normal humans, which was consistent with the previously reported results [35]. Therefore, the aptasensor can provide a clear judgment about whether the human urinary adenosine is at a normal or abnormal level for the clinical diagnosis of lung cancer.

Conclusions

We have successfully developed a dual-emission ratiometric fluorescent aptasensor platform for detection of adenosine with highly sensitive and selective. The contribution of this work is significant for the following reasons: (1) the design of dual-emission ratiometric fluorescent aptasensor can effectively reduce the interference of background and the fluctuation of experimental conditions by built-in calibration of two emission peaks, which can greatly improve the accuracy of response and the reproducibility of measurement; (2) the method can achieve a high sensitivity to adenosine down to 2.4 nM and have more excellent selective binding ability to adenosine than other nucleoside analogs; and (3) the dual-emission ratiometric fluorescent aptasensor provides a dosage-sensitive consecutive color variation from red to royalblue for visual detection of adenosine compared with the single-emission aptasensor. It is believed that the monitoring of adenosine in urine is a practicable and noninvasive method for the diagnosis of disease such as lung cancer.

Acknowledgements This work is supported by the National Natural Science Foundation of China (Nos. 21775073 and 61605084), Natural Science Foundationn of the Jiangsu Higher Education Institutions of China (No. 16KJB150029) and Science and Technology Funds of Nanjing Medical University (No. 2015NJMUZD023).

Compliance with ethical standards The author(s) declare that they have no competing interests.

References

1. Huang HL, Shi S, Gao X, Gao RR, Zhu Y, Wu XW, Zang RM, Yao TM (2016) A universal label-free fluorescent aptasensor based on ru complex and quantum dots for adenosine, dopamine and 17β-estradiol detection. Biosens Bioelectron 79:198–204
2. Gao HW, Duan YY, Xi MY, Sun W (2011) Voltammetric detection of guanosine and adenosine using a carbon paste electrode modified with 1-ethyl-3-methylimidazolium ethylsulfate. Microchim Acta 172:57–64
3. Tzeng HF, Hung CH, Wang JY, Chou CH, Hung HP (2006) Simultaneous determination of adenosine and its metabolites by capillary electrophoresis as a rapid monitoring tool for 5-nucleotidase activity. J Chromatogr A 1129:149–152
4. Huang YF, Chang HT (2007) Analysis of adenosine triphosphate and glutathione through gold nanoparticles assisted laser desorption/ionization mass spectrometry. Anal Chem 79:4852–4859
5. Zhang C, Man BY, Jiang SZ, Yang C, Liu M, Chen CS, Xu SC, Qiu HW, Li Z (2015) SERS detection of low-concentration adenosine by silver nanoparticles on silicon nanoporous pyramid arrays structure. Appl Surf Sci 347:668–672
6. Lin YX, Zhou Q, Tang DP, Niessner R, Knopp D (2017) Signal-on photoelectrochemical immunoassay for aflatoxin B1 based on enzymatic product-etching MnO_2 nanosheets for dissociation of carbon dots. Anal Chem 89:5637–5645
7. Song HY, Kang TF, Jiang MF, Zhang JJ, Cheng SY (2017) A novel strategy based on DNAzyme for electrochemiluminescence detection of Pb(II) with P-GO@QDs for signal amplification. Electroanal Chem 801:244–250
8. Zhu L, Xu GH, Song Q, Tang T, Wang X, Wei FD, Hu Q (2016) Highly sensitive determination of dopamine by a turn-on fluorescent biosensor based on aptamer labeled carbon dots and nanographite. Sensors Actuators B Chem 231:506–512
9. Chen XQ, Chen SF, Hu TY, Ma Q (2017) Fluorescent aptasensor for adenosine based on the use of quaternary CuInZnS quantum dots and gold nanoparticles. Microchim Acta 184:1361–1367
10. Zhu S, Meng Q, Wang L, Zhang J, Song Y, Jin H, Zhang K, Sun H, Wang H, Yang B (2013) Highly photoluminescent carbon dots for multicolor patterning, snsors, bioimaging. Angew Chem Int Ed 52:3953–3957
11. Zhang K, Zhou H, Mei Q, Wang S, Guan G, Liu R, Zhang J, Zhang Z (2011) Instant visual detection of trinitrotoluene particulates on various surfaces by ratiometric fluorescence of dual-emission quantum dots hybrid. J Am Chem Soc 133:8424–8427
12. Huang XY, Zhou YJ, Liu C, Zhang RL, Zhang LY, Du SH, Liu BH, Han MY, Zhang ZP (2016) A single dual-emissive nanofluorophore test paper for highly sensitive colorimetry-based quantification of blood glucose. Biosens Bioelectron 86:530–535
13. Zhao HM, Chang YY, Liu M, Gao S, Yu HT, Quan X (2013) A universal immunosensing strategy based on regulation of the interaction between graphene and graphene quantum dots. Chem Commun 49:234–236
14. Abd El-sadek MS, Kumar JR, Moorthy Babu S (2010) The role of potassium tellurite as tellurium source in mercaptoacetic acid-capped CdTe nanoparticles. Curr Appl Phys 10:317–322
15. Li HH, Zhu HJ, Sun MT, Yan YH, Zhang K, Huang DJ, Wang SH (2015) Manipulating the surface chemistry of quantum dots for sensitive ratiometric fluorescence detection of sulfur dioxide. Langmuir 31:8667–8671
16. Mohapatra S, Sahu S, Nayak S, Ghosh SK (2015) Design of Fe_3O_4@SiO_2@carbon quantum dot based nanostructure for fluorescence sensing, magnetic separation, and live cell imaging of fluoride ion. Langmuir 31:8111–8120
17. Li PJ, Hong YY, Feng HT, Li SFY (2017) An efficient "off–on" carbon nanoparticle-based fluorescent sensor for recognition of chromium(VI) and ascorbic acid based on the inner filter effect. J Mater Chem B 5:2979–2988
18. Zu FL, Yan FY, Bai ZJ, Xu JX, Wang YY, Huang YC, Zhou XG (2017) The quenching of the fluorescence of carbon dots: a review on mechanisms and applications. Microchim Acta 184:1899–1914
19. Chang HX, Tang LH, Wang Y, Jiang JH, Li JH (2010) Graphene fluorescence resonance energy transfer aptasensor for the thrombin detection. Anal Chem 82:2341–2346
20. Freeman R, Girsh J, Willner I (2013) Nucleic acid/quantum dots (QDs) hybrid Systems for Optical and Photoelectrochemical Sensing. ACS Appl Mater Interfaces 5:2815–2834
21. Song E, Cheng D, Song Y, Jiang M, Yu J, Wang Y (2013) A graphene oxide-based FRET sensor for rapid and sensitive detection of matrix metalloproteinase 2 in human serum sample. Biosens Bioelectron 47:445–450
22. Weng X, Neethirajan S (2016) A microfluidic biosensor using graphene oxide and aptamer-functionalized quantum dots for peanut allergen detection. Biosens Bioelectron 85:649–656
23. Wang X, Xu GH, Wei FD, Ma YS, Ma YJ, Song YY, Cen Y, Hu Q (2017) Highly sensitive and selective aptasensor for detection of adenosine based on fluorescence resonance energy transfer from carbon dots to nano-graphite. J Colloid Interface Sci 508:455–461
24. Xu ZQ, Lan JY, Jin JC, Gao T, Pan LL, Jiang FL, Liu Y (2015) Mechanistic studies on the reversible photophysical properties of carbon nanodots at different pH. Colloids Surf B: Biointerfaces 130:207–214
25. Bai YF, Feng F, Zhao L, Chen ZZ, Wang HY, Duan YL (2014) A turn-on fluorescent aptasensor for adenosine detection based on split aptamers and graphene oxide. Analyst 139:1843–1846
26. Shen X, Xu L, Zhu WY, Li BZ, Hong JL, Zhou XM (2017) A turn-on fluorescence aptasensor based on carbon dots for sensitive detection of adenosine. New J Chem 41:9230–9235
27. Cheng X, Cen Y, Xu G, Wei F, Shi M, Xu X, Sohail M, Hu Q (2018) Aptamer based fluorometric determination of ATP by exploiting the FRET between carbon dots and graphene oxide. Microchim Acta 185:144
28. Song Y, Xu G, Wei F, Cen Y, Sohail M, Shi M, Xu X, Ma Y, Ma Y, Hu Q (2018) Aptamer-based fluorescent platform for ultrasensitive adenosine detection utilizing Fe3O4 magnetic nanoparticles and silver nanoparticles. Microchim Acta 185:139
29. Liu X, Lin B, Yu Y, Cao Y, Guo M (2018) A multifunctional probe based on the use of labeled aptamer and magnetic nanoparticles for fluorometric determination of adenosine 5′-triphosphate. Microchim Acta 185:243
30. Kong C, Gao L, Chen Z (2018) Colorimetric adenosine aptasensor based on DNA cycling amplification and salt-induced aggregation of gold nanoparticles. Microchim Acta 185:488
31. Liu JB, Liu Y, Yang XH, Wang KM, Wang Q, Shi H, Li L (2013) Exciton energy transfer-based fluorescent sensing through aptamer-programmed self-assembly of quantum dots. Anal Chem 85:11121–11128
32. Chen SJ, Huang YF, Huang CC, Lee KH, Lin ZH, Chang HT (2008) Colorimetric determination of urinary adenosine using aptamer-modified gold nanoparticles. Biosens Bioelectron 34:1749–1753
33. Kloor D, Yao KZ, Delabar U, Osswald H (2000) Simple and sensitive binding assay for measurement of adenosine using reduced s-adenosylhomocysteine hydrolase. Clin Chem 46:537–542
34. Sun JW, Jiang W, Zhu J, Li W, Wang L (2015) Label-free fluorescence dual-amplified detection of ddenosine based on exonuclease III-assisted DNA cycling and hybridization chain reaction. Biosens Bioelectron 70:15–20
35. Xu G, Schmid HR, Lu X, Liebich HM, Lu P (2000) Excretion pattern investigation of urinary normal and modified nucleosides of breast cancer patients by RP-HPLC and factor analysis method. Biomed Chromatogr 14:459–463